

Self-Consistent Quantum Master Equation Approach to Molecular Transport[†]

Massimiliano Esposito[‡] and Michael Galperin^{*,§}

Center for Nonlinear Phenomena and Complex Systems, Université Libre de Bruxelles, CP 231, Campus Plaine, B-1050 Brussels, Belgium, and Department of Chemistry & Biochemistry, University of California at San Diego, La Jolla, California 92093

Received: April 14, 2010; Revised Manuscript Received: June 16, 2010

We propose a self-consistent generalized quantum master equation (GQME) to describe electron transport through molecular junctions. In a previous study [Esposito, M.; Galperin, M. *Phys. Rev. B* **2009**, *79*, 205303], we derived a time-nonlocal GQME to cure the lack of broadening effects in Redfield theory. To do so, the free evolution used in the Born–Markov approximation to close the Redfield equation was replaced by a standard Redfield evolution. In the present paper, we propose a backward Redfield evolution leading to a time-local GQME which allows for a self-consistent procedure of the GQME generator. This approach is approximate but properly reproduces the nonequilibrium steady-state density matrix and the currents of an exactly solvable model. The approach is less accurate for higher moments such as the noise.

1. Introduction

Recent advances in the experimental capabilities for constructing molecular junctions and measuring their response to external perturbations create new challenges for an adequate theoretical description of open quantum systems far from equilibrium.^{1–4} In molecular junctions, most of the interesting applications are concerned with either strongly correlated or resonant tunneling regimes (or both). In these situations, conventional perturbation theory and/or effective mean-field theories (e.g., Hartree–Fock, GW, DFT) are inapplicable and may lead to unphysical predictions.⁵

In molecular junctions, molecules are sensible to processes such as oxidation, reduction, and excitations. This makes the description of transport in the language of the many-body states of the isolated molecules a convenient tool for molecules weakly coupled to the contacts. Furthermore, sophisticated quantum chemistry methods use many-body states to describe molecular electronic structures.⁶ The dressed state representation,⁷ often employed in quantum chemistry, is another example of many-body states formulation. The standard nonequilibrium Green function (NEGF) approach^{8–10} is formulated in the language of elementary excitations and is therefore not well suited for a many-body states description. A suitable alternative, the Hubbard NEGF approach,^{11–13} still displays inconsistencies for the low level of approximation that need to be resolved (see ref 13 for a discussion).

The simplest approach to transport at the molecular-state level is the Redfield quantum master equation (QME) originally developed in the context of NMR¹⁴ and later in many other fields^{7,15,16} including transport through quantum junctions.^{17–20} It is derived using the Born–Markov approximation in order to get a closed evolution equation for the reduced density matrix. The rotating wave (or secular) approximation (RWA)^{15,18} is often invoked when the molecular levels are well separated so that the molecule Bohr frequencies evolve fast compared to the relaxation time scale induced by the coupling to the contact.

This leads to a QME which has a simple physical interpretation in the molecular eigenbasis. Indeed, populations satisfy a rate equation with rates given by the Fermi golden rule (Pauli equation), and the coherences are each independently exponentially damped. As a result, in nonequilibrium steady states, all coherence effects (in the molecular eigenbasis) are lost. In its general form, the Markovian Redfield equation predicts steady-state coherences that can be inaccurate and even sometimes lead to unphysical results.^{18,21–23} Furthermore, the broadening effects of the molecular levels due to the coupling to the contacts are absent in the Redfield description, that is, the molecular levels are infinitely narrow. Approximate schemes to incorporate the latter in the QME description have been proposed in refs 24–27. In order to overcome some of these difficulties, we proposed in our previous work²⁷ a generalized QME capable of predicting the broadening of the molecular levels in an approximate way. The key idea was to replace the assumption of free molecular evolution inside of the kernel (which is second order in the molecule–contact interaction) used in the Born–Markov approximation by the Redfield evolution. The resulting equation was however nonlocal in time. Here, we extend our consideration by proposing a kind of time-reversed Redfield evolution that leads to a time-local generalized QME. This procedure is rewarding because it allows one to formulate a practical self-consistent scheme to calculate the generator of the QME.

It is well known that formally exact (local or nonlocal in time) QME can be derived using Liouville projection operators and that the Redfield equation can be obtained from it using perturbation theory.¹⁵ In the context of quantum junctions, it has been recently shown²⁰ that this exact QME approach is equivalent to the master equation developed in refs 28 and 29 for the charge state probabilities with rates calculated using nonequilibrium Green function diagrammatic techniques. Recently, the later approach was reformulated as a quantum master equation theory in ref 26. Our considerations are much simpler since they exclusively rely on the knowledge of the Redfield propagator obtained at second-order perturbation theory from the formally exact schemes. However, since we combine it with a self-consistent procedure in the time domain, it makes a detailed comparison nontrivial.

[†] Part of the “Mark Ratner Festschrift”.

^{*} To whom correspondence should be addressed.

[‡] Université Libre de Bruxelles.

[§] University of California at San Diego.

Self-consistent procedures are commonly used in Green function formulations of transport but much less in QME formulations, although standard self-consistent Green function schemes have been rewritten in the language of Liouville space.³⁰ Similarly, an infinite hierarchy of the Green function equations of motion was rewritten in the Liouville space language in ref 31. These reformulations rely on the representation of the system (molecular) Hamiltonian in terms of standard second quantized Fermi operators. This provides the full power of the standard diagrammatic techniques but makes the treatment of intrasystem interactions a hard part of the formulation in exactly the same way as with standard Green function methods.

In our approach, the system Hamiltonian is defined in terms of many-body states. This means that all of the interactions within the isolated system in principle can be calculated using appropriate methods, and their effect on the dynamics can be fully taken into account. The price to pay is a more intricate way of treating the system–bath coupling. In molecular junctions, formulation of transport in the language of many-body states of isolated molecule is essential due to molecular sensitivity to oxidation/reduction/excitation. Thus, formulation of the QME in the language of states of an isolated molecule is essential for molecular devices. In particular, it allows a bridge between quantum chemistry and molecular electronics and incorporation of the machinery of equilibrium molecular spectroscopy into a junction setup. We thus hope that our scheme may become a practical approach for realistic ab initio calculations of steady-state transport in molecular junctions. Examples of ab initio simulations successfully combined with many-body states formulations can be found in ref 32 using the Redfield QME and in ref 33 using the Hubbard NEGF approach.

We finally note that it is important to distinguish between strong on-the-molecule correlations (including electron–electron and electron–phonon) and strong correlations between the molecule and the contacts (e.g., Kondo effect). The former are naturally incorporated in any QME approach simply by going to the eigenbasis of the system. The latter effect is essentially nonperturbative in the molecule–contact coupling and thus cannot be treated using QME schemes such as our.

The structure of the paper is the following. Section 2 introduces a model of molecular junction. In section 3, we briefly review our generalized QME derived earlier and introduce the self-consistent scheme. Section 4 presents numerical examples and compares the results obtained within the scheme to a numerically exact approach. Conclusions are drawn in section 5.

2. Model

We consider a molecule (M) coupled to two metal contacts (L and R), each at its own equilibrium. The Hamiltonian of the system is

$$\hat{H} = \hat{H}_M + \sum_{K=L,R} (\hat{H}_K + \hat{V}_{KM}) \quad (1)$$

The contacts are assumed to be reservoirs of free charge carriers

$$\hat{H}_K = \sum_{k \in K} \varepsilon_k \hat{c}_k^\dagger \hat{c}_k \quad (2)$$

where $K = L, R$ and \hat{c}_k^\dagger (\hat{c}_k) are creation (annihilation) operators for an electron in state k .

The molecular Hamiltonian is represented in terms of the many-body states $\{|M\rangle\}$ of the isolated molecule

$$\hat{H}_M = \sum_{M_1, M_2} |M_1\rangle H_{M_1 M_2}^{(M)} \langle M_2| \equiv \sum_{M_1, M_2} H_{M_1 M_2}^{(M)} \hat{X}_{M_1, M_2} \quad (3)$$

where \hat{X}_{M_1, M_2} are projection (or Hubbard) operators. In particular, in the eigenbasis representation, the molecular Hamiltonian reads

$$\hat{H}_M = \sum_M E_M \hat{X}_{M, M} \quad (4)$$

where E_M are the eigenenergies. Note that the molecular many-body states $|M\rangle$ are characterized by all of the relevant quantum numbers describing the state of an isolated molecule or a dressed state.

The coupling between the molecule and the contacts is introduced in the usual way with hopping terms for the electrons moving from the contact to the molecule and vice versa

$$\hat{V}_{KM} = \sum_{k \in K} \sum_{\mathcal{M}} (V_{\mathcal{M}k} \hat{X}_{\mathcal{M}}^\dagger \hat{c}_k + V_{k, \mathcal{M}} \hat{c}_k^\dagger \hat{X}_{\mathcal{M}}) \quad (5)$$

Here

$$\mathcal{M} \equiv (N_f s_f, N_i s_i) \quad (6)$$

is a transition from the molecular state $M_i \equiv N_i s_i$ to the molecular state $M_f \equiv N_f s_f$. The number of electrons on the molecule is $N_f = N_i - 1$ and s_i (s_f) is the set of all of the quantum numbers characterizing the molecular state in the charging block N_i (N_f), so that $\hat{X}_{\mathcal{M}} \equiv \hat{X}_{M_f, M_i}$.

3. Generalized Quantum Master Equation

In this section, we start by reviewing the derivation of the time-nonlocal GQME introduced in our previous work. We then propose a new way to close the master equation by using a time-reversed effective evolution. This allows formulation of a time-local GQME which can be used as the starting point of a self-consistent scheme to calculate the propagator of the molecular density matrix.

Exact Equation of Motion. We start by deriving an exact equation of motion (EOM) for the quantity

$$\langle \hat{X}_{21}(t) \rangle \equiv \text{Tr}[e^{+i\hat{H}(t-t_0)} \hat{X}_{21} e^{-i\hat{H}(t-t_0)} \hat{\rho}_0] \equiv \sigma_{12}(t) \quad (7)$$

where $|1\rangle$ and $|2\rangle$ are many-body molecular states, t_0 is a starting point of the evolution usually taken at the infinite past $t_0 \rightarrow -\infty$, and $\hat{\rho}_0$ is the initial density operator for the whole system (molecule and contacts). We note that

$$\sigma_{12}(t) \equiv \langle 1 | \text{Tr}_K [\hat{\rho}(t)] | 2 \rangle \quad (8)$$

is a matrix element of the reduced density operator of the molecule $\hat{\sigma}$ at time t , which is obtained by tracing out the contact degrees of freedom from the full density matrix.

The Heisenberg EOM for the Hubbard operator in eq 7 yields an exact EOM for the reduced density matrix (see ref 27 for details of the derivation), which in the molecular eigenbasis reads

$$\begin{aligned}
\frac{d}{dt}\sigma_{12}(t) = & -i(E_1 - E_2)\sigma_{12}(t) - \sum_{\mathcal{M}} \sum_s \int_{-\infty}^t dt' \\
& i\{(-1)^{N_1-N_2}[\sum_{\mathcal{M}(N_1-1s,1)}^{\leftarrow}(t-t')\langle\hat{X}_{\mathcal{M}}(t')\hat{X}_{N_1-1s,2}^\dagger(t)\rangle \\
& + \langle\hat{X}_{N_2-1s,1}(t)\hat{X}_{\mathcal{M}}^\dagger(t')\rangle\sum_{\mathcal{M}(N_2-1s,2)}^{\leftarrow}(t'-t)] \\
& - \sum_{\mathcal{M}(2N_2+1s)}^{\leftarrow}(t-t')\langle\hat{X}_{\mathcal{M}}(t')\hat{X}_{1,N_2+1s}^\dagger(t)\rangle \\
& + \langle\hat{X}_{\mathcal{M}}^\dagger(t)\hat{X}_{N_2-1s,1}(t)\rangle\sum_{\mathcal{M}(N_2-1s,2)}^{\rightarrow}(t'-t) \\
& + \sum_{\mathcal{M}(N_2-1s,1)}^{\rightarrow}(t-t')\langle\hat{X}_{N_1-1s,2}(t)\hat{X}_{\mathcal{M}}(t')\rangle \\
& - \langle\hat{X}_{2,N_1+1s}(t)\hat{X}_{\mathcal{M}}^\dagger(t')\rangle\sum_{\mathcal{M}(1,N_1+1s)}^{\leftarrow}(t'-t) \\
& - (-1)^{N_1-N_2}[\sum_{\mathcal{M}(2N_2+1s)}^{\rightarrow}(t-t')\langle\hat{X}_{1,N_2+1s}^\dagger(t)\hat{X}_{\mathcal{M}}(t')\rangle \\
& + \langle\hat{X}_{\mathcal{M}}^\dagger(t')\hat{X}_{2,N_1+1s}(t)\rangle\sum_{\mathcal{M}(1,N_1+1s)}^{\rightarrow}(t'-t)] \quad (9)
\end{aligned}$$

Here, \mathcal{M} is defined in eq 6, $\sum_{\mathcal{M}_1, \mathcal{M}_2}^{\leftarrow(\rightarrow)}$ are the greater (lesser) projections of a self-energy due to the coupling to the contacts

$$\sum_{\mathcal{M}_1, \mathcal{M}_2}(\tau_1, \tau_2) \equiv \sum_{K=L,R} \sum_{k \in K} V_{\mathcal{M}_1 k} g_k(\tau_1, \tau_2) V_{k, \mathcal{M}_2} \quad (10)$$

where $g_k(\tau_1, \tau_2) \equiv -i\langle T_c \hat{c}_k(\tau_1) \hat{c}_k^\dagger(\tau_2) \rangle$ is the free electron Green function (T_c is the contour ordering operator). Langreth projection rules¹⁰ are applied to get lesser and greater projections from the contour expression of the self-energy eq 10.

A dissipation matrix Γ is introduced in a usual way

$$\Gamma_{\mathcal{M}_1, \mathcal{M}_2}(E) = i[\sum_{\mathcal{M}_1, \mathcal{M}_2}^{\leftarrow}(E) - \sum_{\mathcal{M}_1, \mathcal{M}_2}^{\rightarrow}(E)] \quad (11)$$

It will later be assumed energy-independent (wide band approximation). We also note that as usual in QME and Green function theories, the initial density matrix of the system (at infinite past) is assumed to be a direct product of system (molecule) and bath (contacts) density matrices.

Equation 9 is exact but does not have a closed form in terms of the reduced density matrix σ_{12} . Indeed, its right-hand side contains two-time correlation functions of Hubbard operators. An attempt to write EOM for the latter would lead to expressions having on their right-hand side correlation functions of higher order involving both molecular Hubbard operators and creation (annihilation) operators for the electrons in the contacts at different times. This would generate an infinite hierarchy of EOMs.

Generalized Time-Nonlocal QME. In statistical mechanics, equations of motion for reduced n -body quantities are known to lead to infinite hierarchies which can be closed by approximately representing higher-order quantities in terms of lower-order ones. In particular, closing eq 9 for the case when \mathcal{M} are effective single-particle orbitals at the first step (i.e., reducing the two-time correlation function on the right-hand side to a single time average) is known as the generalized Kadanoff–Baym ansatz (GKBA).¹⁰ In our previous work,²⁷ we introduced the analogue of the GKBA in Liouville space where \mathcal{M} are single electron transitions between many-body states

$$\begin{aligned}
\langle\hat{X}_{12}(t)\hat{X}_{34}^\dagger(t')\rangle \approx & i \sum_{M_1, M_2} [\tilde{\mathcal{G}}_{12, M_1, M_2}^{\leftarrow}(t-t')\langle\hat{X}_{M_1, M_2}(t')\hat{X}_{34}^\dagger(t')\rangle - \\
& \langle\hat{X}_{12}(t)\hat{X}_{M_1, M_2}^\dagger(t)\rangle\tilde{\mathcal{G}}_{M_1, M_2, 34}^{\rightarrow}(t-t')] \quad (12)
\end{aligned}$$

A similar expression holds for $\langle\hat{X}_{34}^\dagger(t')\hat{X}_{12}(t)\rangle$. Here $\mathcal{G}^{r(a)}$ are retarded (advanced) Green functions in Liouville space

$$\begin{aligned}
\mathcal{G}_{12,34}^r(t) & \equiv -i\theta(t)\langle\langle\hat{X}_{21}\hat{I}_B e^{-i\mathcal{L}t}|\hat{X}_{43}\hat{\rho}_B^{\text{eq}}\rangle\rangle \\
& \equiv -i\theta(t)\langle\langle\hat{X}_{21}e^{-i\mathcal{L}_{\text{eff}}t}|\hat{X}_{43}\rangle\rangle \quad (13)
\end{aligned}$$

$$\begin{aligned}
\mathcal{G}_{12,34}^a(t) & \equiv -i\theta(-t)\langle\langle\hat{X}_{34}\hat{I}_B e^{i\mathcal{L}t}|\hat{X}_{12}\hat{\rho}_B^{\text{eq}}\rangle\rangle \\
& \equiv i\theta(-t)\langle\langle\hat{X}_{34}e^{i\mathcal{L}_{\text{eff}}t}|\hat{X}_{12}\rangle\rangle \quad (14)
\end{aligned}$$

where $\hat{\rho}_B^{\text{eq}} \equiv \hat{\rho}_L^{\text{eq}}\hat{\rho}_R^{\text{eq}}$ is the equilibrium density operator for the contacts and \hat{I}_B is the unity operator in the contact subspace. Using eq 12 in eq 9 leads to a time-nonlocal generalized QME given by eq 35 in ref 27.

Generalized Time-Local QME. We now propose an alternative way to close eq 9 by reducing the two-time correlation function on the right-hand side of eq 9 to the later rather than earlier time. Indeed, because the whole system evolution is time-reversible (one has to be careful with spin and magnetic fields, though) and because the reduction of a two-time correlation function to a single-time average is an approximation, the reduction of the correlation function to a later time does not a priori seem to be worse than that to the earlier one.

The two-time correlation function can be exactly expressed in Liouville space as

$$\begin{aligned}
\langle\hat{X}_{12}(t)\hat{X}_{34}^\dagger(t')\rangle = & \theta(t-t')\langle\langle\hat{X}_{34}\hat{I}_B e^{-i\mathcal{L}(t-t')}|\hat{\rho}(t)\hat{X}_{12}\rangle\rangle + \\
& \theta(t'-t)\langle\langle\hat{X}_{12}^\dagger\hat{I}_B e^{-i\mathcal{L}(t-t')}|\hat{X}_{34}^\dagger\hat{\rho}(t')\rangle\rangle \quad (15)
\end{aligned}$$

Then, using the projection superoperator introduced in ref 27

$$\mathcal{P} = \sum_{M_1, M_2} |\hat{X}_{M_1, M_2}\hat{\rho}_B^{\text{eq}}\rangle\langle\langle\hat{X}_{M_1, M_2}\hat{I}_B| \quad (16)$$

one gets the alternative ansatz

$$\begin{aligned}
\langle\hat{X}_{12}(t)\hat{X}_{34}^\dagger(t')\rangle \approx & i \sum_{M_1, M_2} [\tilde{\mathcal{G}}_{12, M_1, M_2}^{\leftarrow}(t-t')\langle\hat{X}_{M_1, M_2}(t')\hat{X}_{34}^\dagger(t')\rangle - \\
& \langle\hat{X}_{12}(t)\hat{X}_{M_1, M_2}^\dagger(t)\rangle\tilde{\mathcal{G}}_{M_1, M_2, 34}^{\rightarrow}(t-t')] \quad (17)
\end{aligned}$$

and a similar expression for $\langle\hat{X}_{34}^\dagger(t')\hat{X}_{12}(t)\rangle$. Here, we introduced the retarded and advanced Green functions on the Keldysh anticontour³⁴

$$\begin{aligned}
\tilde{\mathcal{G}}_{12,34}^r(t) & \equiv -i\theta(-t)\langle\langle\hat{X}_{21}\hat{I}_B e^{-i\mathcal{L}t}|\hat{X}_{43}\hat{\rho}_B^{\text{eq}}\rangle\rangle \\
& \equiv -i\theta(-t)\langle\langle\hat{X}_{21}e^{-i\theta\mathcal{L}_{\text{eff}}t}|\hat{X}_{43}\rangle\rangle \quad (18)
\end{aligned}$$

$$\begin{aligned}
\tilde{\mathcal{G}}_{12,34}^a(t) & \equiv i\theta(t)\langle\langle\hat{X}_{34}\hat{I}_B e^{i\mathcal{L}t}|\hat{X}_{12}\hat{\rho}_B^{\text{eq}}\rangle\rangle \\
& \equiv i\theta(t)\langle\langle\hat{X}_{34}e^{i\theta\mathcal{L}_{\text{eff}}t}|\hat{X}_{12}\rangle\rangle \quad (19)
\end{aligned}$$

where $\theta\mathcal{L}_{\text{eff}}$ is the effective Liouvillian generating the time-reversed evolution. Its connection to the effective Liouvillian \mathcal{L}_{eff} generating forward-time evolution is^{35,36}

$$\theta\mathcal{L} = \mathcal{L}^* \quad (20)$$

Note the difference in sign with refs 35 and 36, which is due to our definition of the evolution operator as $e^{-i\mathcal{L}_{\text{eff}}t}$ instead of $e^{\theta_{\text{eff}}t}$ in refs 35 and 36.

Applying eq 17 to eq 9 leads to a time-local version of the generalized QME

$$\frac{d}{dt}\sigma_{12}(t) = -i \sum_{3,4} \mathcal{L}_{12,34} \sigma_{34}(t) \quad (21)$$

where in the molecular eigenbasis

$$\begin{aligned} -i\mathcal{L}_{12,34} = & -i(E_1 - E_2)\delta_{1,3}\delta_{2,4} - \sum_{\mathcal{M}} \int_{-\infty}^{+\infty} dt \\ & \{(-1)^{N_1-N_2}\delta_{N_1-1,N_3}\delta_{N_2-1,N_4} \times \\ & [\tilde{\mathcal{G}}_{(3,1),\mathcal{M}}^a(t)\Sigma_{\mathcal{M}(4,2)}^<(t) - \Sigma_{(3,1),\mathcal{M}}^<(t)\tilde{\mathcal{G}}_{\mathcal{M}(4,2)}^r(-t)] \\ & - (-1)^{N_1-N_2}\delta_{N_1+1,N_3}\delta_{N_2+1,N_4} \times \\ & [\tilde{\mathcal{G}}_{(2,4),\mathcal{M}}^a(t)\Sigma_{\mathcal{M}(1,3)}^>(-t) - \Sigma_{(2,4),\mathcal{M}}^>(t)\tilde{\mathcal{G}}_{\mathcal{M}(1,3)}^r(-t)] + \\ & \delta_{1,3}\delta_{N_2,N_4} \sum_s [\tilde{\mathcal{G}}_{(N_2-1s,4),\mathcal{M}}^a(t)\Sigma_{\mathcal{M}(N_2-1s,2)}^>(-t) + \\ & \Sigma_{(2,N_2+1s),\mathcal{M}}^<(t)\tilde{\mathcal{G}}_{\mathcal{M}(4,N_2+1s)}^r(-t)] - \\ & \delta_{2,4}\delta_{N_1,N_3} \sum_s [\tilde{\mathcal{G}}_{(3,N_1+1s),\mathcal{M}}^a(t)\Sigma_{\mathcal{M}(1,N_1+1s)}^<(-t) + \\ & \Sigma_{(N_1-1s,1),\mathcal{M}}^>(t)\tilde{\mathcal{G}}_{\mathcal{M}(N_1-1s,3)}^r(-t)] \quad (22) \end{aligned}$$

Note that this expression for the effective Liouvillian in an arbitrary basis will differ from eq 22 only in the free evolution term. Equation 21 reduces to the Markovian Redfield QME when the Green functions eqs 18 and 19 are replaced by their free evolution counterparts, that is, when effective Liouvillian in their definition is substituted by the free system evolution Liouvillian.

It should be clear from our derivation that the time-local form eq 21 of the generalized QME should have a similar degree of accuracy as the time-nonlocal version proposed earlier.²⁷ However, the present form is more suitable for realistic calculations, but most important, it naturally suggests a self-consistent procedure to evaluate the effective Liouvillian. Indeed, the effective Liouvillian, eq 22, depends on the Liouville space Green functions, eqs 18 and 19, which in turn depend on the Liouvillian through the connection eq 20.

Time-local formulation is convenient for treating steady-state situations, while time-nonlocal formulation is preferable for study of time-dependent and transient phenomena. In the latter case, one needs to evolve Liouville space Green functions, eqs 13 and 14, which in general will contain T -ordered exponents in their definition. Here, we focus on the steady-state situation and time-local formulation. The steady-state density matrix is given by the right eigenvector of the nondissipative mode of the Liouvillian.

Expression for Current. The general expression for the time-dependent current at the contact–molecule interface K can be calculated within the nonequilibrium Hubbard Green function approach as^{13,37}

$$I_K(t) = 2 \text{Im} \int_{-\infty}^t dr' \sum_{\mathcal{M},\mathcal{M}'} [\langle \hat{X}_{\mathcal{M}}(t)\hat{X}_{\mathcal{M}'}^\dagger(r') \rangle \Sigma_{\mathcal{M}\mathcal{M}'}^<K(t'-t) + \langle \hat{X}_{\mathcal{M}'}^\dagger(r')\hat{X}_{\mathcal{M}}(t) \rangle \Sigma_{\mathcal{M}\mathcal{M}'}^>K(t'-t)] \quad (23)$$

Using our ansatz, eq 17, leads to the expression

$$\begin{aligned} I_K(t) = & -2 \text{Re} \int_{-\infty}^{+\infty} dt' \sum_{\mathcal{M},\mathcal{M}'} \sum_s \\ & [\sigma_{N_s,N_{s'}}(t)\tilde{\mathcal{G}}_{(N_s,N+1s),\mathcal{M}}^a(t-t')\Sigma_{\mathcal{M}\mathcal{M}'}^<K(t'-t) \\ & + \sigma_{N+1s,N+1s'}(t)\tilde{\mathcal{G}}_{(N_{s'},N+1s),\mathcal{M}'}^a(t-t')\Sigma_{\mathcal{M}'\mathcal{M}}^>K(t'-t)] \quad (24) \end{aligned}$$

where $\mathcal{M} \equiv (N_{S_F}, N + 1s_i)$.

Full Counting Statistics. The theory of full counting statistics (FCS) was initially proposed by Levitov and Lesovik^{38,39} and became popular in the molecular electronics community when shot noise in molecular junctions became experimentally measurable.⁴⁰ The theoretical formalism for FCS within the QME was developed in ref 41. Within the FCS, the evolution operator is dressed by the counting field(s) λ , which tracks the exchange of electrons between the molecule and the contact(s)

$$\hat{V}_{\text{KM}}^\lambda = \sum_{k \in K} \sum_{\mathcal{M}} (V_{\mathcal{M}k} e^{i\lambda/2} \hat{X}_{\mathcal{M}}^\dagger \hat{c}_k + V_{k\mathcal{M}} e^{-i\lambda/2} \hat{c}_k^\dagger \hat{X}_{\mathcal{M}}) \quad (25)$$

Below, we assume that the counting starts at time t_0 .

The dressed Liouville equation for the total density matrix takes the form

$$|\hat{\rho}_\lambda(t)\rangle\rangle = \exp[-i\mathcal{L}_\lambda^\lambda(t-t_0)]|\hat{\rho}(t_0)\rangle\rangle \quad (26)$$

As usual, the initial condition is assumed to be a direct product of the molecular and bath density matrices

$$|\hat{\rho}(t_0)\rangle\rangle = |\hat{\sigma}(t_0)\hat{\rho}_B^{\text{eq}}\rangle\rangle \quad (27)$$

so that the dressed evolution of the system DM becomes

$$|\hat{\rho}_\lambda(t)\rangle\rangle = \exp[-i\mathcal{L}_{\text{eff},\lambda}^\lambda(t-t_0)]|\hat{\sigma}(t_0)\rangle\rangle \quad (28)$$

The FCS is given by the generating function

$$G(t, \lambda) \equiv \langle\langle \hat{I}|\hat{\rho}_\lambda(t)\rangle\rangle \quad (29)$$

The long time limit of the logarithm of the generating function

$$S(\lambda) \equiv \lim_{t \rightarrow \infty} \frac{1}{t} \ln G(t, \lambda) \quad (30)$$

provides information on the steady-state cumulants of the FCS

$$C_n \equiv \frac{d^n}{d(i\lambda)^n} S(\lambda) \quad (31)$$

In particular, the steady-state current is given by the first cumulant, and the second cumulant yields to the zero-frequency shot noise. Using the spectral decomposition of the effective Liouvillian

$$\mathcal{L}_{\text{eff},\lambda} = \sum_{\gamma} |R_{\gamma}(\lambda)\rangle v_{\gamma}(\lambda) \langle L_{\gamma}(\lambda)| \quad (32)$$

and because in the long time limit only the slowest eigenmode $v_0(\lambda)$ survives, we get

$$I = - \left. \frac{dv_0(\lambda)}{d\lambda} \right|_{\lambda=0} \quad (33)$$

$$S = i \left. \frac{d^2 v_0(\lambda)}{d\lambda^2} \right|_{\lambda=0} \quad (34)$$

We note that both eqs 24 and 33 provide the same steady-state current.

4. Numerical Examples

As discussed in the Introduction, a formulation of transport in the language of many-body states is crucial for the study of molecular junctions in the resonance tunneling regime. This is naturally achieved when using standard QME such as the Redfield QME since all on-molecule interactions can, in principle, be included in the many-body eigenenergies. Our approach retains this strength but improves the way coupling to the bath is treated. It is, however, intentionally tested below on a noninteracting system in order to allow comparison with exact NEGF results.

We now compare the results predicted by our new self-consistent approach with the standard Markovian Redfield equation and the nonequilibrium Green function results. The simplest model which can be treated by these three methods, while providing information on both populations and coherences, is a noninteracting two-level bridge (TLB) between metallic contacts.

The bridge part of the model has four many-body states, $|0\rangle \equiv |0, 0\rangle$, $|a\rangle \equiv |1, 0\rangle$, $|b\rangle \equiv |0, 1\rangle$, and $|2\rangle \equiv |1, 1\rangle$, where $|n_a, n_b\rangle$ indicates number of electrons $n_{a,b} = \{0, 1\}$ on the levels a and b, respectively. The relevant single-electron transitions \mathcal{M} are $(0, a)$, $(0, b)$, $(b, 2)$, and $(a, 2)$. They are connected to the second quantized (single-particle) excitation operators used in standard GF approaches by

$$\hat{d}_a = \hat{X}_{0a} + \hat{X}_{b2} \quad (35)$$

$$\hat{d}_b = \hat{X}_{0b} - \hat{X}_{a2} \quad (36)$$

where $\hat{d}_{a,b}^\dagger$ ($\hat{d}_{a,b}$) are the creation (annihilation) operators for an electron on levels a and b, respectively.

The molecular Hamiltonian, eq 3, in this case takes the form

$$\hat{H}_M = \varepsilon_a \hat{X}_{aa} + \varepsilon_b \hat{X}_{bb} + t(\hat{X}_{ab} + \hat{X}_{ba}) \quad (37)$$

The model was treated extensively within the QME approach.^{18,42–44}

The TLB model is easily exactly solved using NEGF. The connection of eqs 35 and 36 provides partial information about the many-body state populations but full information about coherences, which makes the comparison between the different approaches meaningful. In particular

$$-iG_{aa}^<(t, t) = \sigma_{00}(t) + \sigma_{bb}(t) \quad (38)$$

$$-iG_{bb}^<(t, t) = \sigma_{00}(t) + \sigma_{aa}(t) \quad (39)$$

$$-iG_{ab}^<(t, t) = \sigma_{ab}(t) \quad (40)$$

Interlevel coherence in the TLB is due to either hopping matrix element t or the coupling of the two levels via a common bath. The latter interference enters through the nondiagonal elements of the bridge–contact coupling matrix

$$\begin{aligned} \Gamma_{ab}^K &\equiv \sum_{k \in K} V_{ak} V_{kb} \delta(E - \varepsilon_k) \\ &\equiv \sum_{k \in K} V_{(0a)k} V_{k(0b)} \delta(E - \varepsilon_k) \end{aligned} \quad (41)$$

$$\equiv - \sum_{k \in K} V_{(b2)k} V_{k(a2)} \delta(E - \varepsilon_k) \quad (42)$$

where $K = L, R$. The matrix is energy-independent in the wide-band limit assumed below. We intentionally perform simulations at low temperature $T = 10$ K to avoid broadening of the bridge levels due to artificially high values of the temperature. We focus on the relevant temperature regime for molecular junctions, $\Gamma \gg k_B T$.

We start our consideration from a simple far-off-resonant case, where $\Gamma_{mn} \ll |\varepsilon_a - \varepsilon_b|$ ($m, n \in \{a, b\}$). Here, our consideration is done in a local molecular basis ($t \neq 0$). The parameters of the calculation are the following: level positions $\varepsilon_a = 0.2$ eV and $\varepsilon_b = 0.5$ eV, interlevel hopping $t = 0.1$, escape rates for both levels into both contacts $\Gamma_{aa}^K = \Gamma_{bb}^K = 0.1$ eV ($K = L, R$), and level mixing due to coupling to the contacts $\Gamma_{ab}^K = \Gamma_{ba}^K = 0.05$ eV. The Fermi energy in the absence of bias is taken as 0, $E_F = 0$, and the voltage division factor is 1, that is, $\mu_L = E_F + |e|V$ and $\mu_R = E_F$. The NEGF calculation is performed on an energy grid spanning the range from -10 to 10 eV with a step of 10^{-4} eV. Both the Redfield QME and our scheme are expected to work properly in this region of parameters. Figure 1 compares the results of the Redfield QME and our new scheme to the exact NEGF results for the model. The main graph and the inset in Figure 1a display populations, eqs 38 and 39. The real part of the coherence, eq 40, is shown in Figure 1b. The imaginary part of the coherence is 0 in this case (not shown). As discussed earlier,²⁷ the Redfield QME approach misses the information about the broadening of the molecular levels. Our approach accurately recovers this information. Both populations and coherence are well-reproduced by our GQME as well as the current–voltage characteristics (see Figure 1c). Qualitatively, the predictions of the Redfield QME approach are also correct here.

We next consider the case of strong mixing due to coupling to the contact(s). Parameters of the calculation are $t = 0$, $\Gamma_{aa}^L = 0.3$ eV, $\Gamma_{aa}^R = 0.048$ eV, $\Gamma_{bb}^L = 0.2$ eV, $\Gamma_{bb}^R = 0.1125$ eV, $\Gamma_{ab}^L = \Gamma_{ba}^L = 0.12$ eV, and $\Gamma_{ab}^R = \Gamma_{ba}^R = 0.15$ eV. The other parameters are the same as those in Figure 1. Figure 2 compares the Redfield QME and our self-consistent GQME scheme with the exact NEGF results. Our scheme still reproduces populations (Figure 2a), coherences (Figure 2b), and current (Figure 2c) accurately. The Redfield QME however fails to reproduce, even qualitatively, the populations (see Figure 2a) and the real part

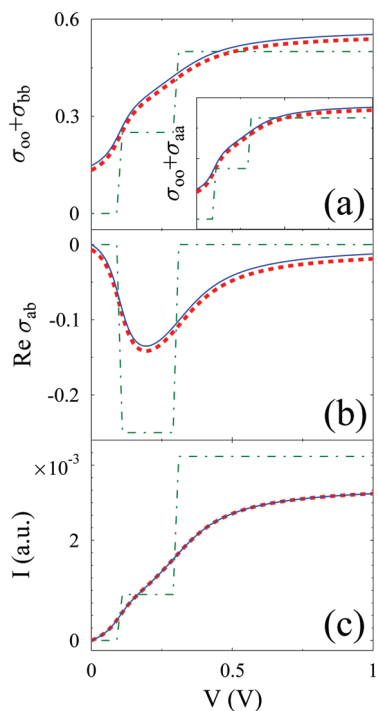


Figure 1. Two-level bridge by Redfield QME (dash–dotted line, green), NEGF (dashed line, red), and self-consistent GQME (solid line, blue) approaches. Shown are (a) probabilities, (b) coherence, and (c) current versus bias. Far-off-resonant local basis treatment. See text for parameters.

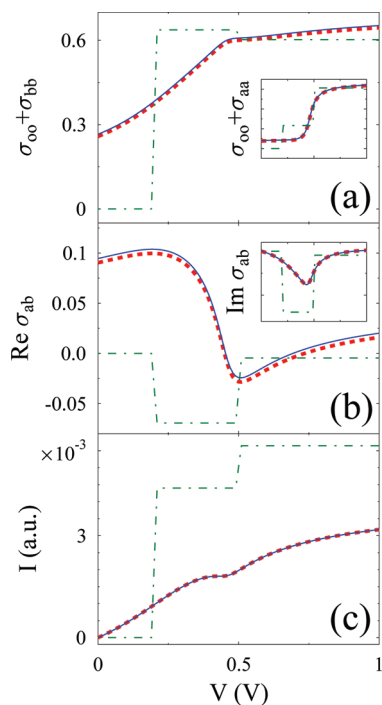


Figure 2. Two-level bridge by Redfield QME (dash–dotted line, green), NEGF (dashed line, red), and self-consistent GQME (solid line, blue) approaches. Shown are (a) probabilities, (b) coherence, and (c) current versus bias. Case of strong mixing due to coupling to the contact(s). See text for parameters.

of the coherence (see Figure 2b). This is due to coherence effects through the bath which are not properly captured by the Redfield QME.

Interference effects in molecular systems were observed experimentally for electron transfer⁴⁵ and molecular junction

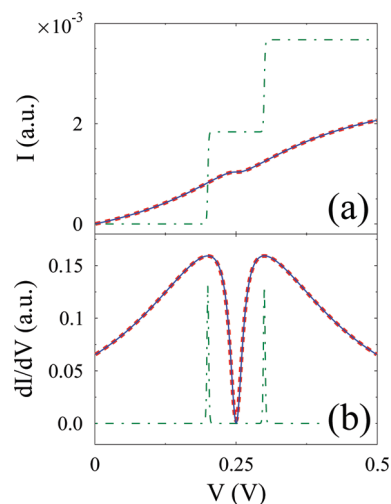


Figure 3. Two-level bridge by Redfield QME (dash–dotted line, green), NEGF (dashed line, red), and self-consistent GQME (solid line, blue) approaches. Shown are (a) current and (b) conductance versus bias. Resonant, $\varepsilon_a = \varepsilon_b$, consideration in a local basis with only level a coupled to contacts, $\Gamma_{aa}^K \neq 0$ and $\Gamma_{bb}^K = \Gamma_{ab}^K = \Gamma_{ba}^K = 0$ ($K = L, R$). See text for parameters.

currents⁴⁶ involving derivatives of benzene connected in the meta or para position. They were also extensively discussed in the theoretical literature.^{47–52} Figure 3 shows the current (a) and conductance (b) versus bias for a model system in which destructive interferences can be experimentally observed and which has been discussed earlier in the literature.⁵² This model is a two-level system with only one of the levels, a, attached to both L and R contacts. The other level, b, is coupled to the level a through a hopping element t . Level b is not directly attached to any contacts. As a result, the tunneling electron has two possible pathways to be transferred from contact L to contact R via the system, one directly through level a and the other by exploring level b on its way. Interference between the two paths leads to a destructive interference in the transport characteristics, which reveals itself as a dip in the conductance. Parameters of the calculation are $\varepsilon_a = \varepsilon_b = 0.25$ eV, $t = 0.05$ eV, $\Gamma_{aa}^L = \Gamma_{aa}^R = 0.2$ eV, and $\Gamma_{ab}^K = \Gamma_{ba}^K = \Gamma_{bb}^K = 0$. Figure 3b shows that the destructive interference in conductance is accurately captured by our self-consistent GQME approach but not by the Redfield QME.

Finally, we present the results of calculation for the zero-frequency shot noise. The shot noise was calculated using the FCS approach, which for the Redfield QME and our self-consistent scheme yields to expression eq 34. The FCS within NEGF was discussed in our previous publication.⁵³ Note that the FCS for a two-level bridge within QME was also discussed in ref 43. We intentionally consider two independent levels (no coupling either within the system or through the bath) to demonstrate the general problem that usual QME schemes have in representing higher moments. We assume that the level $\varepsilon_a = 0.5$ eV is coupled symmetrically to both contacts $\Gamma_{aa}^L = \Gamma_{aa}^R = 0.1$ eV. The other level $\varepsilon_b = 1.5$ eV is coupled asymmetrically $\Gamma_{bb}^L = 10\Gamma_{bb}^R = 0.1$ eV. Other parameters are $t = 0$, $\Gamma_{ab}^K = \Gamma_{ba}^K = 0$, and $T = 10$ K.

Figure 4 compares the results of the Redfield QME and the self-consistent GQME with the exact results provided by NEGF. It is known⁵⁴ that the differential shot noise yields a two-peak structure for a symmetrically coupled molecule, with only a single peak observed for highly asymmetric coupling. One sees that the latter peak (centered at around 1.5 eV in Figure 4b) is reproduced quite well by our self-consistent approach. The

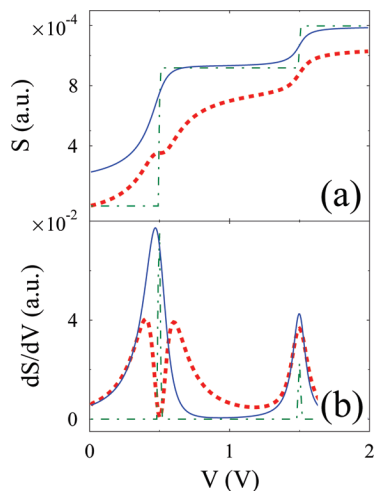


Figure 4. Two-level bridge by Redfield QME (dash–dotted line, green), NEGF (dashed line, red), and self-consistent GQME (solid line, blue) approaches. Shown are (a) shot noise and (b) differential shot noise versus bias. See text for parameters.

double well structure is however missed by both the Redfield QME and our approach (see peak centered at around 0.5 eV). The failure to reproduce zero-frequency noise seems to be a generic problem of all Markovian (effective) second-order QME FCS schemes. Indeed, some simple algebra shows that instead of the correct expression for shot noise in noninteracting system, $\int dE T(E)[f_L(E) - f_R(E)]^2$, standard Markov QME leads to an expression proportional to $\int dE T(E) \times [1 - \int dE T(E)]$, where $T(E)$ is the energy-resolved transmission probability. Using the standard QME (i.e., in the absence of broadening), $T(E)$ is a delta function, and the two expressions are equivalent. Our approach does consider broadening, thus making problem with the zero-frequency noise calculation within the QME FCS technique obvious. More details on this issue are provided in the Appendix. To use the FCS approach, one has to either include higher (at least fourth) order in the presence of broadening or introduce a time-nonlocal object (e.g., an energy-resolved density matrix).⁵⁵

To summarize the results of this section, we can say that, within our simple two-level model of the molecular junction, the comparison of the proposed self-consistent GQME and the Markovian Redfield QME to the exact results provided by the NEGF shows that the self-consistent GQME is highly accurate even when the Redfield QME fails qualitatively. We find that the self-consistent GQME will only fail in the region of parameters where the interlevel coherence due to the coupling to the contacts in the molecular eigenbasis is bigger than the distance between the molecular eigenstates and is on the order of the molecule–contact coupling strength (i.e., exactly at resonance). As a result, in most relevant practical calculations of steady-state transport in molecular junctions, we expect our approach to be accurate. The ability of the proposed scheme to treat molecular transport in the language of many-body states of the isolated molecule and its ability to properly account for interference effects makes it a valuable practical tool for ab initio calculations of transport in molecular junctions.

5. Conclusion

We present a practical scheme to calculate steady-state transport properties in molecular junctions. The scheme is based on a time-local generalized quantum master equation obtained by closing the exact EOM for Hubbard operators by employing

a time-reversed evolution ansatz on the Keldysh anticontour, similar to generalized the Kadanoff–Baym ansatz introduced in our previous publication. We note that the approximations involved in derivation of the time-local equation are essentially the same as those used previously in our time-nonlocal GQME.²⁷ The time locality of our new GQME allows formulation of a self-consistent scheme to calculate the steady-state molecular density matrix and the current in terms of molecular many-body states. We find that the convergence of the self-consistent method for a simple two-level bridge model is achieved within two iterative steps. The results of our method on this model are compared to the results of the Redfield QME and to exact NEGF results. We demonstrate that our scheme (contrary to the Redfield QME result) properly captures populations and coherences. In particular, destructive interference effects in the molecular devices previously discussed in the literature can now be properly described in the many-body states language, which indicates that our scheme could be a valuable tool for practical ab initio calculations. Indeed, the results of standard electronic structure calculation commonly used in quantum chemistry on isolated molecules can easily be incorporated as an input in our method to calculate steady-state transport properties in molecular junctions. The current–voltage characteristics are very accurately reproduced, and we are able to calculate the molecular device characteristics in the experimentally relevant regime of low temperatures. Note however that many important effects due to strong correlation between the molecule and contacts observed at low temperatures (e.g., Kondo) cannot be reproduced within our scheme. We find that our scheme becomes unreliable in the region of the parameters where coherences in the system eigenbasis (i.e., coherences introduced through nondiagonal elements of molecule–contact coupling matrix Γ) are bigger than the interlevel separation and on the order of the diagonal elements of the molecule–contact coupling matrix Γ .

The formulation of a scheme capable of reproducing higher moments in the presence of broadening and the application of our scheme to time-dependent transport is the goal of future research.

Acknowledgment. M.E. is supported by the Belgian Federal Government (IAP project NOSY). M.G. gratefully acknowledges support of the UCSB (Startup Fund) and the U.S.–Israel Binational Science Foundation.

Appendix

We analyze here the FCS in a model made of a single level coupled to two contacts using our QME approach. With two states, $|0\rangle$ and $|1\rangle$, and one transition, $\mathcal{N} = (0, 1)$, involved, the effective Liouvillian (dressed with the counting field λ at the left contact–molecule interface) is given by

$$i\Gamma \begin{bmatrix} -(n_L + n_R) & (\alpha_L - n_L)e^{-i\lambda} + (\alpha_R - n_R) \\ n_L e^{i\lambda} + n_R & -(1 - n_L - n_R) \end{bmatrix} \quad (43)$$

where $\alpha_K \equiv \Gamma_K/\Gamma$ is an asymmetry factor ($K = L, R$), and

$$n_K \equiv \int_{-\infty}^{+\infty} \frac{dE}{2\pi} A(E) \alpha_K f_K(E) \quad (44)$$

is the population of the level due to coupling to contact $K = L, R$. $A(E) \equiv \Gamma/((E - \varepsilon_0)^2 + (\Gamma/2)^2)$ is the density of states (ε_0 is energy of the level). In the standard Redfield formulation, $A(E) = 2\pi\delta(E - \varepsilon_0)$.

The nondecaying mode of the Liouvillian is

$$\nu_0(\lambda) = \frac{i\Gamma}{2}(-1 + [1 - 4n_L\alpha_R(1 - e^{i\lambda}) - 4n_R\alpha_L(1 - e^{-i\lambda}) + 4n_L n_R((1 - e^{i\lambda}) + (1 - e^{-i\lambda}))^{1/2}]) \quad (45)$$

Its first derivative in the counting field, eq 33, gives the steady-state current

$$I = \Gamma(n_L\alpha_R - n_R\alpha_L) \quad (46)$$

and the second derivative, eq 34, gives the zero-frequency noise

$$S(\omega = 0) = \Gamma(n_L\alpha_R + n_R\alpha_L - 2n_L n_R - 2(n_L\alpha_R - n_R\alpha_L)^2) \quad (47)$$

An important difference between current and noise is the nature of the lowest-order process. While the current is a second-order process in the coupling between contacts and the molecule, noise is of fourth order. This might explain why any (effective) second-order scheme cannot properly reproduce noise. In eq 47, this manifests itself by the presence of the terms $\sim n_K n_K'$, which have contributions of the form $\int dE_1 g_1(E_1) \int dE_2 g_2(E_2)$ instead of the proper contribution $\int dE g_1(E) g_2(E)$ ($g_i(E)$ are some functions of energy). This problem is not obvious in the standard Redfield formulation since broadening is absent $g_i(E) \approx \delta(E - \epsilon_0)$. By dressing the molecular states, our approach calculates n_K and consequently also current properly but makes the problem with calculating noise using a Markovian second-order FCS QME formulation obvious.

To calculate noise properly within the QME approach, one could go to a higher-order QME formulation, for example, we can use a fourth-order Liouvillian as an input in our scheme instead of the Redfieldian used so far. Another approach could try to introduce an energy-resolved density matrix as was done, for example, in ref 55.

References and Notes

- Nitzan, A.; Ratner, M. A. *Science* **2003**, *300*, 1384–1389.
- Lindsay, S. M.; Ratner, M. A. *Adv. Mater.* **2007**, *19*, 23–31.
- Galperin, M.; Ratner, M. A.; Nitzan, A. *J. Phys.: Condens. Matter* **2007**, *19*, 103201.
- Galperin, M.; Ratner, M. A.; Nitzan, A.; Troisi, A. *Science* **2008**, *319*, 1056–1060.
- Spataru, C. D.; Hybertsen, M. S.; Louie, S. G.; Millis, A. J. *Phys. Rev. B* **2009**, *79*, 155110.
- Jensen, F. *Introduction to Computational Chemistry*; John Wiley & Sons, Ltd.: New York, 2007.
- Nitzan, A. *Chemical Dynamics in Condensed Phases*; Oxford University Press: New York, 2006.
- Danielewicz, P. *Ann. Phys.* **1984**, *152*, 239–304.
- Rammer, J.; Smith, H. *Rev. Mod. Phys.* **1986**, *58*, 323–359.
- Haug, H. J. W.; Jauho, A.-P. *Quantum Kinetics in Transport and Optics of Semiconductors*; Springer: New York, 2008.
- Sandalov, I.; Johansson, B.; Eriksson, O. *Int. J. Quantum Chem.* **2003**, *94*, 113–143.
- Fransson, J. *Phys. Rev. B* **2005**, *72*, 075314.
- Galperin, M.; Nitzan, A.; Ratner, M. A. *Phys. Rev. B* **2008**, *78*, 125320.
- Redfield, A. G. *IBM J. Res. Dev.* **1957**, *1*, 19–31.
- Breuer, H.-P.; Petruccione, F. *The Theory of Open Quantum Systems*; Oxford University Press: New York, 2002.
- Gaspard, P.; Nagaoka, M. *J. Chem. Phys.* **1999**, *111*, 5668.
- Li, X.-Q.; Luo, J.; Yang, Y.-G.; Cui, P.; Yan, Y. *Phys. Rev. B* **2005**, *71*, 205304.
- Harbola, U.; Esposito, M.; Mukamel, S. *Phys. Rev. B* **2006**, *74*, 235309.
- Schultz, M. C.; von Oppen, F. *Phys. Rev. B* **2009**, *80*, 033302.
- Timm, C. *Phys. Rev. B* **2008**, *77*, 195416.
- Kohen, D.; Tannor, D. J. *J. Chem. Phys.* **1997**, *107*, 5141.
- Kohen, D.; Marston, C. C.; Tannor, D. J. *J. Chem. Phys.* **1997**, *107*, 5236.
- Ishizaki, A.; Fleming, G. R. *J. Chem. Phys.* **2009**, *130*, 234110.
- Pedersen, J. N.; Wacker, A. *Phys. Rev. B* **2005**, *72*, 195330.
- Ovchinnikov, I. V.; Neuhauser, D. *J. Chem. Phys.* **2004**, *122*, 024707.
- Leijnse, M.; Wegewijs, M. R. *Phys. Rev. B* **2008**, *78*, 235424.
- Esposito, M.; Galperin, M. *Phys. Rev. B* **2009**, *79*, 205303.
- König, J.; Schoeller, H.; Schön, G. *Phys. Rev. Lett.* **1997**, *78*, 4482–4485.
- Schoeller, H. *Lect. Notes Phys.* **2000**, *544*, 137–166.
- Cui, P.; Li, X.-Q.; Shao, J.; Yan, Y. *Phys. Lett. A* **2006**, *357*, 449–453.
- Jin, J.; Zheng, X.; Yan, Y. *J. Chem. Phys.* **2008**, *128*, 234703.
- May, V. *Int. J. Quantum Chem.* **2006**, *106*, 3056–3070.
- Yeganeh, S.; Ratner, M. A.; Galperin, M.; Nitzan, A. *Nano Lett.* **2009**, *9*, 1770–1774.
- Bányai, L. *A Non-Equilibrium Theory of Condensed Matter*; World Scientific: River Edge, NJ, 2006.
- Stenholm, S.; Jacob, M. *Ann. Phys.* **2004**, *310*, 106–126.
- Stenholm, S.; Jacob, M. *J. Mod. Opt.* **2004**, *51*, 841–850.
- Jauho, A.-P.; Wingreen, N. S.; Meir, Y. *Phys. Rev. B* **1994**, *50*, 5528–5544.
- Levitov, L. S.; Lesovik, G. B. *JETP Lett.* **1993**, *58*, 230–235.
- Levitov, L. S.; Lee, H.; Lesovik, G. B. *J. Math. Phys.* **1996**, *37*, 4845–4866.
- Djukic, D.; van Ruitenbeek, J. M. *Nano Lett.* **2006**, *6*, 789–793.
- Esposito, M.; Harbola, U.; Mukamel, S. *Rev. Mod. Phys.* **2009**, *81*, 1665–1702.
- Novotný, T. *Europhys. Lett.* **2002**, *59*, 648–654.
- Esposito, M.; Harbola, U.; Mukamel, S. *Phys. Rev. B* **2007**, *75*, 155316.
- Welack, S.; Esposito, M.; Harbola, U.; Mukamel, S. *Phys. Rev. B* **2008**, *77*, 195315.
- Patoux, C.; Coudret, C.; Launay, J.-P.; Joachim, C.; Gourdon, A. *Inorg. Chem.* **1997**, *36*, 5037–5049.
- Mayor, M.; Weber, H. B.; Reichert, J.; Elbing, M.; von Hänisch, C.; Beckmann, D.; Fichtner, M. *Angew. Chem., Int. Ed.* **2003**, *42*, 5834–5838.
- Stafford, C. A.; Cardamone, D. M.; Mazumdar, S. *Nanotechnology* **2007**, *18*, 424014.
- Goldsmith, R. H.; Wasilewski, M. R.; Ratner, M. A. *J. Am. Chem. Soc.* **2007**, *129*, 13066–13071.
- Solomon, G. C.; Andrews, D. Q.; van Duyn, R. P.; Ratner, M. A. *J. Am. Chem. Soc.* **2008**, *130*, 7788–7789.
- Solomon, G. C.; Andrews, D. Q.; Goldsmith, R. H.; Hansen, T.; Wasilewski, M. R.; van Duyn, R. P.; Ratner, M. A. *J. Am. Chem. Soc.* **2008**, *130*, 17301–17308.
- Solomon, G. C.; Andrews, D. Q.; Hansen, T.; Goldsmith, R. H.; Wasilewski, M. R.; van Duyn, R. P.; Ratner, M. A. *J. Chem. Phys.* **2008**, *129*, 054701.
- Solomon, G. C.; Andrews, D. Q.; van Duyn, R. P.; Ratner, M. A. *ChemPhysChem* **2009**, *10*, 257–264.
- Fransson, J.; Galperin, M. *Phys. Rev. B* **2010**, *81*, 075311.
- Galperin, M.; Nitzan, A.; Ratner, M. A. *Phys. Rev. B* **2006**, *74*, 075325.
- Esposito, M.; Gaspard, P. *Phys. Rev. E* **2007**, *76*, 041134.